Published in final edited form as:
Stem Cells. 2014 September ; 32(9): 2386–2396. doi:10.1002/stem.1731.

Engineering the Human Thymic Microenvironment to Support Thymopoiesis in Vivo

Brile Chung[1,2], **Amélie Montel-Hagen**[1], **Shundi Ge**[1], **Garrett Blumberg**[1], **Kenneth Kim**[1], **Sam Klein**[1], **Yuhua Zhu**[1], **Chintan Parekh**[1,3,4], **Arumugam Balamurugan**[5], **Otto O. Yang**[5,6], and **Gay M. Crooks**[1,4,7,8]

[1]Department of Pathology and Laboratory Medicine, David Geffen School of Medicine, (DGSOM), University of California, Los Angeles (UCLA)

[2]Cancer Immunotherapeutics and Tumor Immunology, City of Hope Comprehensive Cancer Center (current affiliation BC)

[3]Division of Pediatric Hematology/Oncology, Children's Hospital Los Angeles (current affiliation CP)

[4]Department of Pediatrics, DGSOM, UCLA

[5]Department of Medicine, Department of Microbiology, Immunology and Molecular Genetics, and UCLA AIDS Institute, UCLA

[6]AIDS Healthcare Foundation, Los Angeles

[7]Broad Stem Cell Research Center, UCLA

[8]Jonsson Comprehensive Cancer Center, UCLA

Abstract

A system that allows manipulation of the human thymic microenvironment is needed both to elucidate the extrinsic mechanisms that control human thymopoiesis, and to develop potential cell therapies for thymic insufficiency. In this report, we developed an implantable thymic microenvironment composed of two human thymic stroma populations critical for thymopoiesis;

Correspondence should be addressed to G.M.C. (gcrooks@mednet.ucla.edu) Gay M. Crooks, M.B.,B.S. Department of Pathology & Laboratory Medicine David Geffen School of Medicine University of California Los Angeles TLSB 3014, 610 Charles E. Young Drive, East Los Angeles, CA 90095-7239 Ph: (310) 206 0205 Fax: (310) 206 0356.

Competing Interests Authors have no conflict of interests with the presentation of this work

Author contributions: Brile Chung: Conception and design, collection and assembly of data, data analysis and interpretation, manuscript writing.
Amelie Montel-Hagen: Collection and assembly of data, data analysis and interpretation, manuscript writing.
Shundi Ge: Collection of data
Garrett Blumberg: Collection of data
Kenneth Kim: Collection of data
Sam Klein: Collection of data
Yuhua Zhu: Collection of data
Chintan Parekh: Collection of data
Arumugam Balamurugan: Collection of data
Otto O. Yang: Data analysis and interpretation specifically on TCR repertoire
Gay M. Crooks: Conception and design, financial support, data analysis and interpretation, manuscript writing and final approval of manuscript

thymic epithelial cells (TECs) and thymic mesenchyme (TM). TECs and TM from postnatal human thymi were cultured in specific conditions, allowing cell expansion and manipulation of gene expression, prior to re-aggregation into a functional thymic unit. Human CD34+ hematopoietic stem and progenitor cells (HSPC) differentiated into T cells in the aggregates in vitro and in vivo following inguinal implantation of aggregates in immune deficient mice. Cord blood HSPC previously engrafted into murine bone marrow, migrated to implants and differentiated into human T cells with a broad T cell receptor repertoire. Furthermore, lentiviral-mediated expression of vascular endothelial growth factor in TM enhanced implant size and function, and significantly increased thymocyte production. These results demonstrate an in vivo system for the generation of T cells from human HSPC, and represent the first model to allow manipulation of gene expression and cell composition in the microenvironment of the human thymus.

Keywords

Thymus; Thymic microenvironment; T-cell development; Thymus transplantation; VEGF; Tissue engineering

Introduction

Thymic dysfunction results from the inability of the thymic microenvironment to generate T lymphocytes in sufficient numbers, functional diversity and specificity. The T cell defects that result from thymic dysfunction render patients highly susceptible to infections, malignancies and/or autoimmune disease. In addition to the thymic involution that occurs with aging, damage to thymic epithelial cells (TECs) can be caused by many external insults including infection, radiation, immunosuppressant therapy, and graft versus host disease after hematopoietic stem cell transplantation [1-5]. In children with Di George syndrome, the thymus fails to develop and severe T cell deficiency can result in lethal infections and autoimmune disease [6]. An experimental model to study how human T cell development is regulated within the human thymic microenvironment is needed to advance our understanding of thymic insufficiency. In addition, progress toward thymic transplantation as a therapeutic option will require methods by which the thymic tissue can be manipulated *ex vivo* to remove endogenous T cells and to maintain the stromal components required to control normal thymopoiesis.

Over the last few decades, several immune deficient murine models have been generated that support the in vivo transplantation and differentiation of human hematopoietic stem and progenitor cells (HSPCs) [7-10]. In the earliest model (the “SCID-hu” mouse), direct implantation of human fetal thymus, liver and bone marrow under the renal capsule of SCID mice produced a transient wave of human T lymphopoiesis *in vivo* [11]. The subsequent adoption of pre-transplant irradiation and administration of human cytokines, produced models that allowed engraftment of more clinically relevant postnatal sources of human HSPC into the murine marrow after intravenous administration [12, 13]. However, these early bone marrow transplantation models supported predominantly B lymphoid differentiation with little or no human T cell development [10]. The development of even

more immune deficient animals, particularly those with null mutations of Interleukin-2 receptor gamma (NOD-SCID IL-2R$\gamma^{-/-}$ and Rag2$^{-/-}$IL-2R$\gamma^{-/-}$), allowed both high level engraftment of human HSPC in the murine bone marrow and T cell differentiation in the endogenous mouse thymus [14-18].

With the goal of providing a human thymic microenvironment for *in vivo* T cell differentiation in engrafted animals, recent modifications have combined the above approaches to create the so-called BLT (bone marrow, liver, thymus) mouse [19]. In this model, intravenously administered human HSPC engrafted in the murine bone marrow after sublethal irradiation are able to migrate to human fetal thymus/ liver tissue implanted under the renal capsule; T cell differentiation in the human thymus is provided by both fetal thymocytes and, after 14-20 weeks, by allogeneic postnatal HSPC which migrate from the marrow [20-22]. Although all of these models have been profoundly important for the experimental study of hematopoiesis and T cell function, none allow the study or manipulation of the thymic microenvironment, and none provide a pathway to develop a translational method for thymic engineering and transplantation.

The goal of the current study was to develop an *in vivo* model of human thymopoiesis in which the compartments of the human thymic microenvironment, and consequently T cell development, can be manipulated. We demonstrate an approach in which *ex vivo* expanded TECs and thymic mesenchyme (TM) derived from human postnatal thymus, and depleted of endogenous thymocytes, can be aggregated into three-dimensional structures and implanted to provide an environment able to support robust thymopoiesis from endogenous human HSPC recruited from the marrow.

In previous studies, we have shown that VEGF produced by the neonatal murine thymic microenvironment induces exuberant angiogenesis, and is critical for thymic growth during the neonatal period [23, 24]. In the current studies, lentiviral mediated local expression of VEGF in the aggregates enhanced their size and function. Moreover VEGF allowed robust vascularization after implantation under the quadriceps muscle sheath, a surgical approach with direct translational application. The human thymic aggregate system can thus be used to study the recruitment of postnatal human HSPC from bone marrow to the thymus, and subsequent in vivo differentiation of T cells. The scale-up of this approach would also offer a potentially clinically relevant method for transplantation of T cell depleted postnatal thymus. Moreover, we provide proof-of-principle that signals from the thymic microenvironment can be engineered with this method, opening up potential applications for the control of T cell growth, differentiation and function within the thymus.

Materials and Methods

Culture of human thymic epithelial cells and thymic mesenchyme

Human TECs and TM were generated from post-natal thymic samples removed as waste tissue from patients (ages ranging from 10 days to 5 months) during cardiothoracic surgery, and provided without patient identifiers, according to guidelines approved by the UCLA Institutional Review Board. Over 20 biological replicates from different donors were used for this study. Thymic tissue was dissociated into fragments (≤ 1 mm diameter) via

mechanical dissociation and plated directly onto 0.1% gelatin coated culture flasks. In subsequent experiments, attachment and expansion of thymic fragments was improved byplating onto Vitrogen (Advanced BioMatrix) coated culture flasks.

To generate TECs in culture, thymic fragments were cultured in calcium-free Dulbecco's modified Eagle's medium (DMEM)/F12 medium (Invitrogen, Grand Island, NY) supplemented with 1% fetal bovine serum (FBS), cholera toxin (10 ng/ml) (Sigma-Aldrich, St Louis, MO), bovine insulin (3 μg/ml) (Sigma-Aldrich), hydrocortisone (0.5 μg/ml) (Sigma-Aldrich), epidermal growth factor (20 ng/ml) (Sigma-Aldrich), penicillin/ streptomycin (Invitrogen), and L-glutamine (Invitrogen) [25]. For the generation of human thymic mesenchyme, thymic fragments were cultured in (DMEM) supplemented with 10% FBS (D10 medium), penicillin/streptomycin (Invitrogen), and L-glutamine (Invitrogen). TM cultures could be passaged several times for up to at least 6 weeks and could also be frozen for later use while maintaining their mesenchyme-specific markers. TEC cultures were not passaged and were typically used after approximately 3 weeks. This time point gave the highest percentage of TECs with fewest CD45+ cells. Longer cultures resulted in a lower percentage of TECs and an increase of the percentage of TMs.

Transduction of Thymic Mesenchyme

The lentiviral vector CClc-TRE-VEGF-PGK-tTA (provided as a gift by Dr. Donald Kohn at UCLA), was used to express human VEGF in the absence of tetracycline. Vector was pseudotyped using vesicular stomatitis virus (VSV) envelope by transient transfection into 293T cells, and concentrated by ultrafiltration and ultracentrifugation as described previously [26]. Thymic mesenchyme cultured for 3 weeks was transduced by the addition of CClc-TRE-VEGF-PGK-tTA (final conc. 1×10^7 infectious units/ml) in the presence of 4 mg/mL of protamine sulfate for 24 hours. Production of human VEGF was measured by using an enzyme-linked immunosorbent assay (ELISA) kit for detection of human VEGF (R&D Systems, Minneapolis, MN).

Generation of human thymic aggregates

Cord Blood was obtained from normal deliveries at UCLA under guidelines approved by UCLA IRB, and CD34+ were isolated to 95% purity by magnetic bead technology (Miltenyi, Auburn CA). To generate each human thymic aggregate, approximately 1×10^5 human TECs, 5×10^4 human TM, and 2×10^5 cord blood-derived CD34+ cells were mixed together in PBS (Mediatech, Inc, Manassas, VA) and centrifuged at 1300rpm for 5 minutes into an aggregate pellet in a microcentrifuge tube (TEC:TM:CD34+ ratio of 2:1:4). Following removal of the supernatant, the aggregate was carefully drawn into a micropipette tip (no more than 10μl volume) and released onto the surface of a nucleopore filter membrane (0.8 μm pores; Millipore, Billerica, MA) floating on gelfoam (Pharmacia & Upjohn, Bridgewater, NJ) in D10 medium supplemented with fms-like tyrosine kinase 3 receptor ligand (FLT3-L: 5 ng/ml; PeproTech, Rocky Hill, NJ), recombinant human interleukin 7 (rhIL-7) (5 ng/ml; R&D Systems), and stem cell factor (SCF) (1 ng/ml; Amgen, Thousand Oaks, CA). The thymic aggregate was then harvested after 2 to 4 weeks in culture for analysis of in vitro thymopoiesis. For the in vivo model, thymic aggregates

were cultured for 24 hours on a nucleopore membrane before implantation in the inguinal area of NSG mice.

Implantation of human thymic aggregates

All in vivo experiments were performed using NOD/SCID/IL-2γc$^{-/-}$ recipients (NSG) mice (Jackson Laboratories, Bar Harbor, ME), kept in separate pathogen-free facilities consistent with the NIH Guide for the Care and Use of Laboratory Animals and under approved protocols of the UCLA Institutional Animal Care and Use Committee. Thymic aggregates were implanted into eight to ten week old NSG mice, under general anesthesia as follows. The skin of the anterior of the thigh was lifted with a pair of blunt forceps and cut along the midline creating an incision approximately an inch in length. The dermis was separated from the underlying body wall on both sides of the incision. A pair of fine forceps was used to gently pinch and lift the fatty tissues covering the deep sections of the thigh muscles near the femoral artery. Each thymic aggregate (approximately 1 mm in diameter) was removed from the nucleopore membrane and gently placed in the inguinal area next to the femoral artery and medial to the quadriceps muscle. Following implantation, the fatty and skin tissues were gently eased back into the body cavity, covering the implanted human thymic aggregate.

Flow Cytometry analysis

Human thymic aggregates were harvested from implanted mice five weeks after implantation. Single cell suspensions of each aggregate were prepared by mechanical dissociation, and the total cell numbers were determined. Approximately 1×10^5 cells were incubated with conjugated antibodies directed against human CD3, CD4, CD5, CD8, CD34, CD45, TCRαβ, HLA-A2, CD1A, CD7, or isotype control monoclonal antibodies (all from BD Pharmingen, San Diego, CA). For analyses of human cultured TECs and TM, cells were harvested with TripLE Select (Gibco) and incubated with conjugated antibodies directed against anti-human CD326 (EP-CAM), PDGFR-α, CD73, CD166, CD105, and CD44, and then washed and analyzed on a FACS LSRII analyzer (BD Biosciences).

Gene expression analyses

RNA was isolated using an RNeasy Micro kit (QIAGEN, Valencia, CA). For real time quantitative PCR (RT-qPCR) assays, cDNAs were prepared using the QuantiTech reverse transcription kit (QIAGEN) and qPCR was performed with LightCycler 480 SYBR Green I Master (Roche) using the LightCycler 480 real-time PCR system (Roche). Cycling conditions consisted of a denaturation step for 15 min at 95°C, followed by 40 cycles of denaturation (95°C for 15 s), annealing (59°C for 20 s) and extension (72°C for 15 s). After amplification, melting curve analysis was performed with denaturation at 95°C for 5 s and continuous fluorescence measurement from 70°C to 95°C at 0.1°C/s. All the samples were normalized to HPRT. The following primers were used: *HPRT* (5′-AACCTCTCGGCTTTCC-3′ [forward], 5′-GCTGCGGGTCGCCATAA-3′ [reverse]), *EPCAM* (5′-AAATGTGTGTGCGTGGGAC-3′ [forward], 5′-GGTAAAGCCAGTTTCAAGC-3′ [reverse]), *KRT5* (5′-ATGGACAACAACCGCAACC-3′ [forward], 5′-GATACCAGGACTCGGCTTCT-3′[reverse]), *KRT14* (5′-TTCGCACCAAGAACTGAGG-3′[forward], 5′-GCTGTATTGATTGCCAGGAGGG-3′

[reverse]), *FGF7* (5′-TGGACACACAACGGAGGG-3′[forward], 5′-CATAGGAAGAAAGTGGGCTG-3′[reverse]), *FGF10* (5′-GCTGAAGGAGAGGATAGAGGAA-3′[forward], 5′-TGGAAGAAAGTGAGCAGAGGTGT-3′[reverse]), *FGFR2* (5′-TTTCATCTGCCTGGTCGTGGTCA-3′[forward], 5′-CTTCTGGCTCTAATGTGGTATCCTC-3′[reverse]), *PDGFRα* (5′-GCTTTCATTACCCTCTATCCTTCC-3′[Forward], 5′-GCTCACTTCACTCTCCC-3′ [Reverse]), *AIRE* (5′ –GCGGGAGAGGAGGTAAGAGG-3′ [Forward], 5′-TCAGGACCCACACACAGTAGG-3′ [Reverse]), *FOXN1* (5′-GCTGCTCGTCATTTGTGT-3′ [Forward], 5′-GGATACTTGTCTGAGGGTG-3′ [Reverse]), *DLL4* (5′-GCCCAAATCAGAAAGGAGAGAGG-3′ [Forward], 5′-AGCAAGAGACGCACCCAGT-3′ [Reverse]), *TP63* (5′-ACTGCTTCCCTTACTTTGCTG-3′ [Forward], 5′-ACCCTGGCTACTCATACACTCA-3′ [Reverse]).

For semi-quantitative PCR assays, first-strand cDNA synthesis was performed using the Omniscript III reverse-transcription–polymerase chain reaction (RT-PCR) kit (QIAGEN). Total cDNA from 5×10^3 to 1×10^4 cells was interrogated for human gene expression with the following primers: *RAG-1* (5′-TTTAAGCTGTTCCGGGTGAG-3′ [forward] and 5′ GGGCTTTTAACAATGGCTGA-3′ [reverse]). *DNTT* (5′-TCTCCCAGTATGCGTGTCAG-3′ [forward] and 5′-GCAGGGAATTCCTTCTGTGT-3′ [reverse]). *PTCRA* (5′-TCCAGCCCTACCCACAGGTG-3′ [forward] and 5′-TAGAAGCCTCTCCTGACAGATGCAT-3′[reverse]). *B2M* (5′-CTCGCGCTACTCTCTCTTTC-3′ [forward] and 5′-CATGTCTCGATCCCACTTAAC-3′ [reverse]). PCRs used HotStar Taq polymerase (QIAGEN) and consisted of 35 to 40 cycles of 30 seconds at 95°C, 30 seconds at 60°C, and 1 minute at 72°C, with a final elongation cycle of 7 minutes at 72°C.

Histology and immunofluorescent microscopy

Thymic aggregates were harvested following euthanasia and embedded in paraffin and fixed in 10% buffered formalin (Sigma-Aldrich). Serial histological sections (5 μm) were incubated for 4hrs at room temperature with rabbit anti-CD31 (Abcam, Cambridge, MA), goat anti-huAIRE (Abcam), rabbit anti-huDLL4 (Abcam) and mouse anti-huCytokeratin (DAKO, Carpinteria, CA) for 4 hours (at dilution 1:400), followed by incubation with biotinylated secondary antibodies (anti-goat, anti-rabbit, or anti-mouse). Labeled tyramide fluorescence alexa fluo 594 or 488 dyes were used for single or multiple staining. All the immunofluorescent images were acquired using the Zeiss axiomager (Thornwood, NY) with Apotome Imaging System, and H&E images were acquired using the Olympus M2 IX51 with DP72 camera (Olympus America Inc, Center Valley, PA) and cell lens standard imaging software.

Analyses of human TCRV beta distribution

A modified TCR spectratyping was performed as previously described in detail [27]. Briefly, human thymocytes from thymic aggregates harvested 35 days post-implantation were removed by mechanical dissociation, and the total RNA was isolated by Trizol/Stat 60

reagent (Invitrogen), followed by reverse transcription (RT) reaction using random hexamer primers. TCR −V_β specific PCR reactions were performed for 24 TCR −V_β complementarity determining region 3 (CDR3) families. For each reaction, one specific V_β forward primer along with fluorescent labeled (6-FAM) TCRβ constant region (5′–CTTCTGATGGCTCAAACAC – 3′) reverse primer was used to amplify a fragment spanning each CDR3 region and quantitate relative concentrations of each family. Size distributions were measured through capillary electrophoresis system on an ABI-3130 analyzer, and analyzed using Genemapper software (Applied Biosystem,Carlsbad CA).

Statistical Analyses

Numbers of total cells and immunophenotypic sub-populations recovered from thymic implants were analyzed using the two- tailed t test with unequal distributions. P value < .05 was considered statistically significant.

Results

1. Generation of human thymic epithelial and mesenchymal cultures

To develop a system that allows manipulation of components of the thymic microenvironment, specific culture conditions that preferentially support the separate *ex vivo* growth of human thymic epithelium and thymic mesenchyme were established using modifications of protocols developed for *in vitro* murine aggregates [28]. Human postnatal thymus tissue from patients ranging from ages 10 days to 5 months was mechanically dissociated into thymic fragments and plated directly into culture flasks in two separate conditions: medium optimal for growth of TECs (which included l% fetal calf-serum, insulin, cholera toxin and epidermal growth factor), and medium with higher amounts of fetal calf serum allowing for more robust growth of TM. Over the next 1-3 weeks, monolayers dominated by the typical morphology of TECs or TM were generated in each respective culture condition and continued to expand approximately 150 fold and 50 fold respectively by outgrowth from the adherent fragments that had been initially plated (Figure 1A).

Successful establishment and maintenance of epithelial monolayers in TEC conditions requires the presence, albeit at low frequency, of residual mesenchymal cells retained from the initial fragments. Immuno-phenotypic characterization of the monolayers generated in TEC cultures after 3 weeks demonstrated more than 40-80% of cells continued to express Epithelial Cell-adhesion molecule (EPCAM, CD326) a cell surface marker expressed by TECs prior to culture, most of which were marked by Ulex Europaeus Agglutinin-1 (UEA-1), a lectin that has been used to identify murine medullary (m)TECs [29, 30] but which appears to be less TEC-specific in human thymus (Figure1B). Typically, CD45+ hematopoietic cells, if detectable at all, represented less than 1% of cells in TEC cultures, representing a two log T cell depletion. Mesenchymal cells persisted at a low frequency in TEC cultures (1-15% of CD45− cells expressed CD105 at 3 weeks of culture, n=4 independent experiments). In contrast, almost all the cells generated in TM culture conditions expressed the mesenchymal markers, CD73, CD105, CD166, CD44, and PDGFRα (Figure 1C).

Quantitative RT-PCR analysis of TECs (CD45-EPCAM+CD105− cells) and TM (CD45-EPCAM-CD105+ cells) isolated from TEC and TM conditions respectively demonstrated that the epithelial genes *EPCAM*, *KRT5* (aka Cytokeratin 5, CK5), *KRT14* (CK14) and *TP63* (p63) were almost exclusively expressed by TECs, as were more TEC-specific regulatory genes *FOXN1* (Forkhead Box N1), *AIRE* (Autoimmune regulator) and *DLL4* (Delta-Like 4). In contrast the mesenchymal marker *PDGFRα* (Alpha-type platelet-derived growth factor receptor) was specifically expressed by TMs. Genes for ligands produced by thymic mesenchyme *FGF7* (Fibroblast Growth Factor 7) and *FGF10* were expressed predominantly in TM cells (Fig 1D), and *FGFR2*, the receptor to which they bind, was expressed predominantly by TECs [31-33] (Figure 1D), providing evidence that cultured TECs can respond to these key mesenchyme-derived growth factors.

2. Generation of human T cells in aggregates of human TM and TECs

Thymic aggregates were created by co-centrifugation of cells from TEC and TM monolayers, harvested from separate cultures after 3-4 weeks. The ability of the thymic aggregates to provide a suitable microenvironment for T cell development was initially examined *in vitro*, by co-aggregating cord blood CD34+ HSPC with cultured TECs and TM and then culturing the chimeric three-dimensional aggregates on nucleopore filters (Figure 2A). By 2 weeks of aggregate culture, CD34+CD1a+ thymic progenitors could be detected and early T cell differentiation had been initiated as shown by cells expressing CD5, CD7, CD3, CD4+CD8+ (DP), CD4+CD8− (SPCD4) and CD8+CD4−(SPCD8) (Figure 2B). By the end of the fourth week of aggregate culture, further T cell differentiation could be seen with an increase in the frequency of DP, SPCD4, and SPCD8 cells associated with increasing CD3 expression (Figure 2B).

To demonstrate the ability of thymic aggregates to support human T cells *in vivo*, thymic aggregates containing TECs, TM and CD34+ cells were implanted under the sheath of the quadriceps muscle in the inguinal area of adult NOD/SCID/IL2Rγ−/− (NSG) mice. After 5 weeks, animals were euthanized and implants were harvested for further analysis. Human CD45+ cells were identified in the aggregates with CD4+CD8+ and CD7+CD1A+ immunophenotypes, typical of human thymocytes (Figure 2C).

3. Effects of lentiviral-mediated VEGF expression in thymic implants

The ability of the human thymic aggregate system to be genetically engineered was next tested. Based on our previous studies in the neonatal thymus [23, 24], we hypothesized that expression of VEGF within the aggregates would promote thymopoiesis. A lentiviral vector engineered to express human VEGF was thus used to transduce three week old TM cultures. Established TM cultures were transduced with high efficiency (>90%) by 24 hour exposure to high titer lentiviral supernatant. ELISA of supernatant collected from stably transduced and passaged TM detected VEGF levels of 3.5-4ng/ml, 9 to 10 fold higher than endogenous VEGF from non-transduced TM, and 4,000 fold higher than nontransduced fresh human thymocytes.

To test the effect on human thymopoiesis of expressing VEGF in implanted aggregates, VEGF-expressing (or control non-transduced), cultured TM were aggregated as described

with cultured TECs and fresh cord blood CD34+ cells and implanted into NSG mice, again in the inguinal region. The VEGF-expressing thymic aggregates were larger and displayed more robust surrounding vasculature than the non-transduced aggregates (Figure 3A). Of the aggregates at harvest, 65% of VEGF aggregates and 54% control aggregates contained detectable human CD45+ cells. The number of total cells harvested from thymic aggregates that expressed VEGF was significantly greater than that seen in the control group of aggregates ($P< 0.002$) (Figure 3B). RT-PCR analysis of cells harvested from both VEGF and control implanted aggregates confirmed the presence of early stages of human thymocyte differentiation with expression of terminal deoxynucleotidyl transferase gene (*DNTT*), recombination activating gene 1 (*RAG-1*) and pre-TCRα gene (*PTCRA*) [34] (Figure 3C).

In both VEGF-secreting and control aggregates, human CD45+ thymocytes harvested from 5 week implants were predominantly immature CD4+CD8+, CD7+, CD1A+, CD5+ cells (Figure 3D). More mature T cells (SPCD4+CD3+, SPCD8+CD3+, SPCD4+TCRαβ, SPCD8+TCRαβ) were also detected in both control and VEGF thymic aggregates. Expression of VEGF in thymic aggregates increased the numbers of all the sub-populations of human thymocytes at least ten-fold including the immature CD7+CD1A+ and CD4+CD8+ subsets (Figure 3E). Overall, these results show that TEC/TM thymic aggregates provide a suitable microenvironment for human CB CD34+ cells to undergo T cell commitment in vivo and that increasing VEGF expression in TM enhances implant survival and significantly increases thymocyte output in the aggregates.

4. TCR repertoire of human thymocytes generated in implanted aggregates

To investigate whether normal TCR gene rearrangement takes place during T-cell development in the implants, we examined the TCR Vβ chain rearrangement using a PCR-based TCR spectratyping assay in human thymocytes recovered from implanted VEGF-expressing thymic aggregates (Figure 4) [27]; control aggregates did not contain sufficient cells for analysis. The distribution of each TCR Vβ displayed normal Gaussian distribution, indicating polyclonal human TCR development in the implanted human thymic microenvironment.

5. Impact of VEGF expression on the thymic epithelial microenvironment

Histologic analysis of thymic aggregates harvested from NSG mice at 35 days showed that VEGF-expressing implants contained a higher density of thymocytes and demonstrated morphology more typical of normal thymus with clearer cortical-medullary junctions, when compared to control implants (Figure 5A). Immunohistochemistry revealed that a higher density of PECAM+ endothelial cells was present in the VEGF-expressing aggregates compared to the control aggregates (Figure 5B). Corresponding to the morphologic data (Figure 5A), human cytokeratin-expressing TECs were more abundant and organized in the VEGF-expressing aggregates compared to the controls (Figure 5C). The transcription factor AIRE, which plays a critical role for the removal of autoreactive T cells during negative selection [35, 36](Figure 5C), and Delta-like ligand 4 (DLL-4), a notch ligand required for early T lymphopoiesis [37](Figure 5D) were highly expressed in the VEGF-expressing aggregates but little expression was seen in controls. Collectively, these results demonstrate

that VEGF expression in vivo enhances the growth, organization and function of the thymic microenvironment after implantation.

6. Migration and differentiation of endogenous HSPC from bone marrow to thymic implants

In vivo human T lymphopoiesis in the data shown above was derived from CB CD34+ cells that were combined with thymic aggregates before implantation. We next evaluated whether implanted aggregates also have the ability to recruit HSPC from the bone marrow and subsequently allow differentiation into human T lymphocytes. Adult NSG recipients were sub-lethally irradiated and transplanted with CB CD34+ HSPC from a human leukocyte antigen A2+ (HLA-A2+) donor to establish stable marrow engraftment. At 4 weeks post-HSPC transplantation, human thymic aggregates containing TEC, CB CD34+ cells from HLA-A2 negative donors and either control or VEGF TM were implanted into the inguinal region of recipient mice (Figure 6A). At time of aggregate implantation, human HLA-A2+CD45+ cells were detected in the peripheral blood of recipient animals, but consistent with the lack of early T cell development seen when NSG mice are transplanted as adults, none of the human cells expressed the T cell marker CD3 (Figure 6B).

Animals were analysed five weeks after implantation of the thymic aggregates (nine weeks after CB HSPC transplantation). At time of harvest, human HSPC (HLA-A2+ CD45+ CD34+ cells) were detected in murine bone marrow at levels between 6 and 15% of mononuclear cells (Figure 6C). No evidence of human thymopoiesis in the endogenous murine thymus was detectable. However, HLA-A2+ thymocytes were readily detected in the human thymic aggregates and included both DP and more mature SP T cells (Figure 6D). HLA-A2+ donor-derived mature T cells were also detected in the spleen and peripheral blood at similar levels between control and VEGF-expressing animals (Figure 6E). Thus the implanted thymic aggregates allowed both recruitment of thymic precursors into and export of human T cells out of the implants to the periphery. Thymocyte numbers were higher in VEGF-expressing aggregates than in control aggregates ($P<0.05$) (Figure 6F), demonstrating again that the manipulation of gene expression in the implanted thymic microenvironment can alter implant function.

Discussion

Although the development of various types of humanized mice has provided the opportunity to study human hematopoiesis *in vivo* [7, 10], a model that allows the detailed analysis of how the non-hematopoietic cells in the thymus regulate thymopoiesis has not been available. In this study, we developed an implantable three-dimensional model of the human thymic microenvironment consisting of *ex vivo* expanded human TECs and TM. The assembly of these cell types into a functional unit generated human T cells from HSPC with a diverse T cell receptor repertoire. The implanted aggregates demonstrated the ability to recruit hematopoietic progenitor cells from the marrow and subsequently allow differentiation into human T lymphocytes. Importantly, the ability to culture TEC and TM components prior to re-aggregation, allowed manipulation of the cellular composition, gene expression and

function of the thymic microenvironment in the implants. This novel method provides a powerful approach for the study of human T-cell development both *in vitro* and *in vivo*.

The recent establishment of the bone marrow/liver/thymus (BLT) humanized mouse, in which human fetal liver, fetal thymus, and cord blood CD34+ cells are transplanted into an immunodeficient mouse, has provided a useful tool to study human T cell development *in vivo* [7, 9, 10]. However, the use of whole fetal thymic fragments in all such modifications of the original SCID-hu model limits the mechanistic and translational questions that can be asked with this approach. Thymopoiesis from the experimental HSPCs occurs in competition with allogeneic mismatched fetal thymocytes reducing the efficiency of thymic engraftment and making quantitation of T cell output unreliable in the SCID-hu model. Most importantly, the inability to manipulate the cellular and molecular composition of the thymic microenvironment means that these models can only provide a physical site for T cell differentiation of HSPC rather than a method for studying the stromal components that regulate thymopoiesis by experimental manipulation.

It should be noted that the CD34+ purity in the cord blood samples used in the aggregates was only ~90-95%. Thus the possibility cannot be discounted that the mature CD4+ and CD8+ T cells seen in the aggregates were expanded or maintained from contaminating mature T cells from co-transplanted cord blood. Nonetheless, T cell commitment and early stages of thymopoiesis were clearly generated from HSPC, as demonstrated by the CD4+CD8+ (DP) and CD7+CD1a+ immunophenotypic populations typical of thymocytes, and mRNA for *RAG1*, *DNTT* and *PTCRA*, genes expressed only during early stages of T cell differentiation.

Notch signaling is critical for the earliest stages of T cell commitment from HSPC [34]. As expression of notch ligands in TECs is down-regulated during monolayer culture [38], retroviral mediated expression of DLL1 or DLL4 in murine stromal cells (e.g. OP9) has been used as an in vitro method to induce T cell differentiation from HSPC [39, 40]. However, normal thymopoiesis is regulated by a complex system comprised of epithelial, mesenchymal and vascular components in a three-dimensional organ. Studies using cultured murine thymus show that the three dimensional aggregate model is the only in vitro system that can recapitulate the complex interactions of normal thymopoiesis well enough to study such mechanisms as central tolerance [28]. Previous reports of murine thymic aggregates have used fetal thymus [41] and the little success that has been accomplished using postnatal murine TECs has used fetal mesenchyme [42, 43].

The importance of the interactions between TM and TECs for establishing a normal thymic microenvironment for T cell development has been well documented [31-33, 44]. Experimental studies have shown that the TM has essential roles in survival and maturation of TECs, which in turn orchestrate T cell proliferation and differentiation. Key ligands that are known to induce proliferation of TECs (e.g., FGF-7 and FGF-10) are produced by murine thymic mesenchyme, and mutations in FgfR2-IIIb (the receptor for FGF-7 and FGF10) or FGF10 lead to thymic agenesis or hypoplasia [31-33]. The removal of mesenchyme from the murine E12 thymic lobe results in a loss of proliferation and differentiation of TEC, but the development of TEC can be restored by adding back thymic

mesenchyme [45]. In addition, expression of critical ligands (e.g. IL-7, SCF, and notch ligands) by TECs is significantly reduced in the absence of TM [32]. Since the frequency of TM and TECs in the thymus is extremely low, it is likely that each fragment of human fetal thymus implanted in the BLT model consists of variable and sometimes inadequate components of TM and TECs, which with the additional competition with endogenous human fetal thymocytes, can lead to inconsistent experimental results. The aggregate model provides the ability to modify the relative composition of TECs and TM and to further explore the cross-talk mechanisms that allow maintenance, growth and function of the thymic microenvironment. A further benefit of the method is that, during TEC and TM culture, contaminating thymocytes are profoundly depleted.

Thymic implants have been used clinically to treat infants born with complete absence of the thymus (aka complete DiGeorge Anomaly). The risk of graft versus host disease from allo-reactive fetal thymocytes and the logistical difficulties of obtaining fetal thymus for transplantation, has led to the use of postnatal thymic tissue, cultured as intact chunks to remove contaminating thymocytes, and surgically implanted in the muscle sheath [46]. Although this approach has allowed the development of T cells with normal proliferative responses and T cell receptor repertoire, patients have remained severely T lymphopenic and autoimmune disease has developed in approximately 20% of patients [46]. We propose that these clinical outcomes are likely to have occurred because of suboptimal survival and function of TECs, both because of apoptosis of epithelial cells during culture and because of difficulty establishing vascularization throughout the relatively thick thymic chunks.

Use of the thymic aggregate system allows localized production of either membrane bound or secreted regulators in either mesenchyme or epithelium. We have previously shown that high levels of endogenous VEGF in the murine neonatal thymus drives angiogenesis and rapid growth of the organ during the first 4-7 days of postnatal life. Inhibition of VEGF signaling inhibits neonatal thymopoiesis and blocks thymic angiogenesis, but has no effect on the adult thymus [23]. VEGF inhibition in neonatal hosts also delays thymic reconstitution after allogeneic bone marrow transplantation [24]. It is conceivable that one reason for the dependence of the SCID-hu model on fetal tissue may be higher levels of VEGF expression in the fetal than the postnatal thymic mesenchyme. We now show that forced local expression of VEGF in the postnatal human thymic implants significantly improves the T cell output of engrafted implants. VEGF-expressing thymic aggregates were comprised of a more organized thymic morphology with robust DLL-4 expression, and epithelial cells that express AIRE. While the improved T cell output is likely due to survival and function of TECs which in turn may be a consequence of the re-vascularization induced by VEGF, it is also possible that VEGF may stimulate non-endothelial compartments of the thymic microenvironment directly. We propose that the expression of VEGF in these “inter-muscular” implants allows a surgical method that, unlike the renal capsule approach, could be used for clinical thymic transplantation.

In summary, we present evidence that the generation of an implantable human thymic microenvironment provided by TECs and TM from postnatal thymi and engineered to express VEGF can successfully recapitulate de novo human thymopoiesis. The scale-up of this novel experimental model could provide a potential approach for clinical translation as a

method for thymic regeneration and for manipulation of thymic T cell differentiation in vivo.

Acknowledgments

This work was supported by grants from the California Institute of Regenerative Medicine (CIRM) RM1-01707 and National Institutes of Health (P01 HL073104) (GMC), AM-H was supported by an American Society of Hematology Scholar award. CP is a St. Baldrick's Foundation Scholar, and recipient of a CHLA K12 Child Health Research Career Development award and research funds from the Nautica Malibu Triathlon. We gratefully acknowledge the expert technical assistance of the Broad Stem Cell Research Center Flow Cytometry Core and the CFAR Virology Core Lab & Tissue Culture/PCR Facility at UCLA.

References

1. Chung B, Barbara-Burnham L, Barsky L, et al. Radiosensitivity of thymic interleukin-7 production and thymopoiesis after bone marrow transplantation. Blood. 2001; 98:1601–1606. [PubMed: 11520813]
2. Douek DC, McFarland RD, Keiser PH, et al. Changes in thymic function with age and during the treatment of HIV infection. Nature. 1998; 396:690–695. [PubMed: 9872319]
3. Hakim FT, Memon SA, Cepeda R, et al. Age-dependent incidence, time course, and consequences of thymic renewal in adults. J Clin Invest. 2005; 115:930–939. [PubMed: 15776111]
4. Mackall CL, Fleisher TA, Brown MR, et al. Age, thymopoiesis, and CD4+ Tlymphocyte regeneration after intensive chemotherapy. N Engl J Med. 1995; 332:143–149. [PubMed: 7800006]
5. Weinberg K, Blazar BR, Wagner JE, et al. Factors affecting thymic function after allogeneic hematopoietic stem cell transplantation. Blood. 2001; 97:1458–1466. [PubMed: 11222394]
6. Markert ML, Hummell DS, Rosenblatt HM, et al. Complete DiGeorge syndrome: persistence of profound immunodeficiency. J Pediatr. 1998; 132:15–21. [PubMed: 9469994]
7. Brehm MA, Jouvet N, Greiner DL, et al. Humanized mice for the study of infectious diseases. Curr Opin Immunol. 2013
8. Brehm MA, Shultz LD, Greiner DL. Humanized mouse models to study human diseases. Curr Opin Endocrinol Diabetes Obes. 2010; 17:120–125. [PubMed: 20150806]
9. Legrand N, Weijer K, Spits H. Experimental models to study development and function of the human immune system in vivo. J Immunol. 2006; 176:2053–2058. [PubMed: 16455958]
10. Shultz LD, Ishikawa F, Greiner DL. Humanized mice in translational biomedical research. Nat Rev Immunol. 2007; 7:118–130. [PubMed: 17259968]
11. McCune JM, Namikawa R, Kaneshima H, et al. The SCID-hu mouse: murine model for the analysis of human hematolymphoid differentiation and function. Science. 1988; 241:1632–1639. [PubMed: 2971269]
12. Lapidot T, Pflumio F, Doedens M, et al. Cytokine stimulation of multilineage hematopoiesis from immature human cells engrafted in SCID mice. Science. 1992; 255:1137–1141. [PubMed: 1372131]
13. Nolta JA, Hanley MB, Kohn DB. Sustained human hematopoiesis in immunodeficient mice by cotransplantation of marrow stroma expressing human interleukin-3: analysis of gene transduction of long-lived progenitors. Blood. 1994; 83:3041–3051. [PubMed: 7514050]
14. Ishikawa F, Yasukawa M, Lyons B, et al. Development of functional human blood and immune systems in NOD/SCID/IL2 receptor {gamma} chain(null) mice. Blood. 2005; 106:1565–1573. [PubMed: 15920010]
15. Ito M, Hiramatsu H, Kobayashi K, et al. NOD/SCID/gamma(c)(null) mouse: an excellent recipient mouse model for engraftment of human cells. Blood. 2002; 100:3175–3182. [PubMed: 12384415]
16. Lepus CM, Gibson TF, Gerber SA, et al. Comparison of human fetal liver, umbilical cord blood, and adult blood hematopoietic stem cell engraftment in NOD-scid/gammac−/−, Balb/c-Rag1−/−gammac−/−, and C.B-17-scid/bg immunodeficient mice. Hum Immunol. 2009; 70:790–802. [PubMed: 19524633]

17. Pearson T, Shultz LD, Miller D, et al. Non-obese diabetic-recombination activating gene-1 (NOD-Rag1 null) interleukin (IL)-2 receptor common gamma chain (IL2r gamma null) null mice: a radioresistant model for human lymphohaematopoietic engraftment. Clin Exp Immunol. 2008; 154:270–284. [PubMed: 18785974]
18. Traggiai E, Chicha L, Mazzucchelli L, et al. Development of a human adaptive immune system in cord blood cell-transplanted mice. Science. 2004; 304:104–107. [PubMed: 15064419]
19. Wege AK, Melkus MW, Denton PW, et al. Functional and phenotypic characterization of the humanized BLT mouse model. Curr Top Microbiol Immunol. 2008; 324:149–165. [PubMed: 18481459]
20. Kalscheuer H, Danzl N, Onoe T, et al. A model for personalized in vivo analysis of human immune responsiveness. Sci Transl Med. 2012; 4:125ra130.
21. Melkus MW, Estes JD, Padgett-Thomas A, et al. Humanized mice mount specific adaptive and innate immune responses to EBV and TSST-1. Nat Med. 2006; 12:1316–1322. [PubMed: 17057712]
22. Tonomura N, Habiro K, Shimizu A, et al. Antigen-specific human T-cell responses and T cell-dependent production of human antibodies in a humanized mouse model. Blood. 2008; 111:4293–4296. [PubMed: 18270327]
23. Cuddihy AR, Ge S, Zhu J, et al. VEGF-mediated cross-talk within the neonatal murine thymus. Blood. 2009; 113:2723–2731. [PubMed: 19088378]
24. Cuddihy AR, Suterwala BT, Ge S, et al. Rapid thymic reconstitution following bone marrow transplantation in neonatal mice is VEGF-dependent. Biol Blood Marrow Transplant. 2012; 18:683–689. [PubMed: 22281302]
25. Ropke C, Elbroend J. Human thymic epithelial cells in serum-free culture: nature and effects on thymocyte cell lines. Dev Immunol. 1992; 2:111–121. [PubMed: 1379502]
26. Haas DL, Case SS, Crooks GM, et al. Critical factors influencing stable transduction of human CD34(+) cells with HIV-1-derived lentiviral vectors. Mol Ther. 2000; 2:71–80. [PubMed: 10899830]
27. Balamurugan A, Ng HL, Yang OO. Rapid T cell receptor delineation reveals clonal expansion limitation of the magnitude of the HIV-1-specific CD8+ T cell response. J Immunol. 2010; 185:5935–5942. [PubMed: 20944001]
28. Anderson G, Jenkinson EJ. Investigating central tolerance with reaggregate thymus organ cultures. Methods Mol Biol. 2007; 380:185–196. [PubMed: 17876094]
29. Akiyama T, Shimo Y, Yanai H, et al. The tumor necrosis factor family receptors RANK and CD40 cooperatively establish the thymic medullary microenvironment and self-tolerance. Immunity. 2008; 29:423–437. [PubMed: 18799149]
30. Poliani PL, Facchetti F, Ravanini M, et al. Early defects in human T-cell development severely affect distribution and maturation of thymic stromal cells: possible implications for the pathophysiology of Omenn syndrome. Blood. 2009; 114:105–108. [PubMed: 19414857]
31. Dooley J, Erickson M, Larochelle WJ, et al. FGFR2IIIb signaling regulates thymic epithelial differentiation. Dev Dyn. 2007; 236:3459–3471. [PubMed: 17969154]
32. Itoi M, Tsukamoto N, Yoshida H, et al. Mesenchymal cells are required for functional development of thymic epithelial cells. Int Immunol. 2007; 19:953–964. [PubMed: 17625108]
33. Revest JM, Suniara RK, Kerr K, et al. Development of the thymus requires signaling through the fibroblast growth factor receptor R2-IIIb. J Immunol. 2001; 167:1954–1961. [PubMed: 11489975]
34. Spits H. Development of alphabeta T cells in the human thymus. Nat Rev Immunol. 2002; 2:760–772. [PubMed: 12360214]
35. Gardner JM, Fletcher AL, Anderson MS, et al. AIRE in the thymus and beyond. Curr Opin Immunol. 2009; 21:582–589. [PubMed: 19833494]
36. Yano M, Kuroda N, Han H, et al. Aire controls the differentiation program of thymic epithelial cells in the medulla for the establishment of self-tolerance. J Exp Med. 2008; 205:2827–2838. [PubMed: 19015306]
37. Koch U, Fiorini E, Benedito R, et al. Delta-like 4 is the essential, nonredundant ligand for Notch1 during thymic T cell lineage commitment. J Exp Med. 2008; 205:2515–2523. [PubMed: 18824585]

38. Mohtashami M, Zuniga-Pflucker JC. Three-dimensional architecture of the thymus is required to maintain delta-like expression necessary for inducing T cell development. J Immunol. 2006; 176:730–734. [PubMed: 16393955]

39. Schmitt TM, Zuniga-Pflucker JC. Induction of T cell development from hematopoietic progenitor cells by delta-like-1 in vitro. Immunity. 2002; 17:749–756. [PubMed: 12479821]

40. Zuniga-Pflucker JC. T-cell development made simple. Nat Rev Immunol. 2004; 4:67–72. [PubMed: 14704769]

41. Anderson G, Jenkinson EJ, Moore NC, et al. MHC class II-positive epithelium and mesenchyme cells are both required for T-cell development in the thymus. Nature. 1993; 362:70–73. [PubMed: 8446171]

42. Gray D, Abramson J, Benoist C, et al. Proliferative arrest and rapid turnover of thymic epithelial cells expressing Aire. J Exp Med. 2007; 204:2521–2528. [PubMed: 17908938]

43. Seach N, Hammett M, Chidgey A. Isolation, characterization, and reaggregate culture of thymic epithelial cells. Methods Mol Biol. 2013; 945:251–272. [PubMed: 23097111]

44. Jenkinson WE, Rossi SW, Parnell SM, et al. PDGFRalpha-expressing mesenchyme regulates thymus growth and the availability of intrathymic niches. Blood. 2007; 109:954–960. [PubMed: 17008543]

45. Jenkinson WE, Jenkinson EJ, Anderson G. Differential requirement for mesenchyme in the proliferation and maturation of thymic epithelial progenitors. J Exp Med. 2003; 198:325–332. [PubMed: 12860931]

46. Markert ML, Devlin BH, Alexieff MJ, et al. Review of 54 patients with complete DiGeorge anomaly enrolled in protocols for thymus transplantation: outcome of 44 consecutive transplants. Blood. 2007; 109:4539–4547. [PubMed: 17284531]

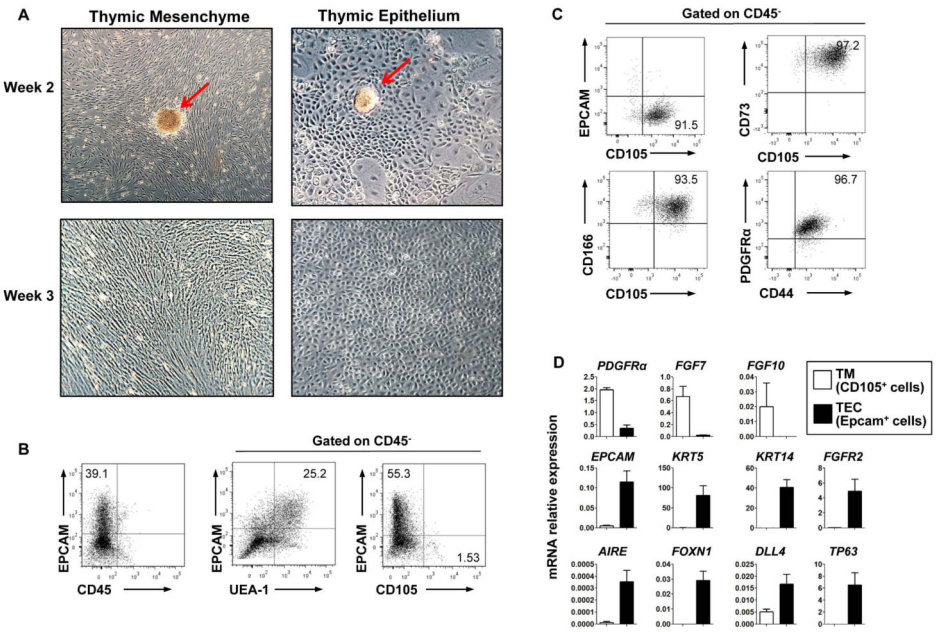

Figure 1. Characterization of human TECs and TM in culture

(**A**) Morphology of hTECs and hTM generated in separate cultures, 2 and 3 weeks after initiation from human thymic fragments (red arrows indicate remaining fragments). (Phase microscopy, 10x magnification). At 2 to 3 weeks, cell surface marker expression was analyzed by FACS on monolayers formed in TEC conditions (**B**) and TM conditions (**C**). In **(B),** (middle and right panel) and in (C), profiles are from CD45− gated cells. (**D**) Quantitative RT-PCR analyses of TECs (EPCAM+CD45-CD105−) and TM (CD45-EPCAM-CD105+) isolated by FACS from TEC and TM cultures respectively, normalized to *HPRT* expression. Data is representative of >20 cultures set up from thymus samples of different donors

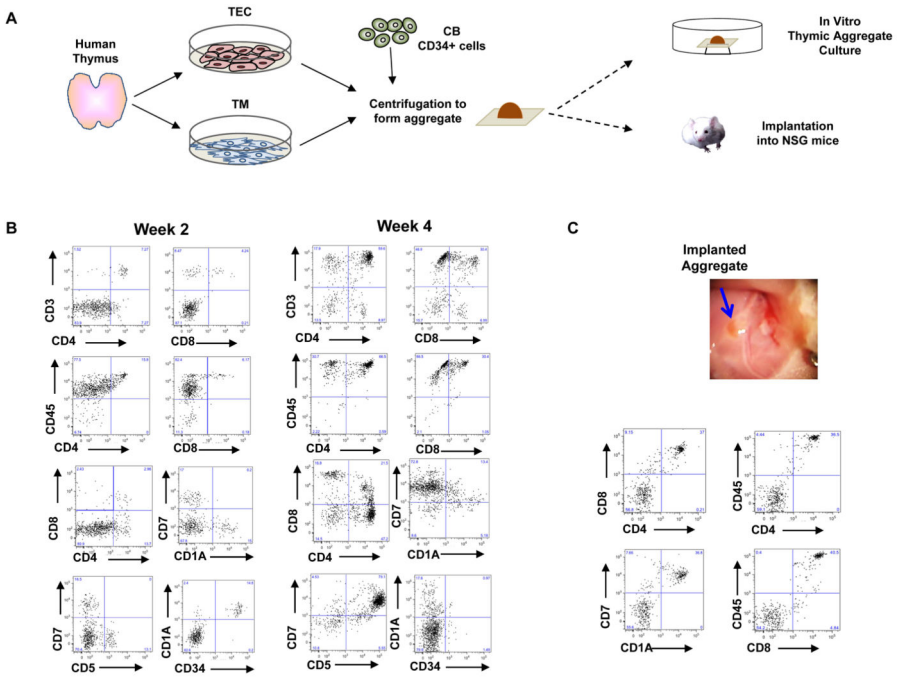

Figure 2. Generation of human T cells in human thymic aggregates *in vitro* and *in vivo*

(**A**) Schematic representation for generation of human thymic aggregates for *in vitro* and *in vivo* models. Human TECs and TM were generated from post-natal thymus (less than 5 months old) *ex vivo*. Cultured human TECs, TM, and fresh cord blood-derived CD34+ cells were centrifuged to form aggregates. Aggregates were then cultured on nucleopore membranes floating in D10 medium supplemented with FLT-3 ligand, IL-7, and SCF, either for 4 weeks for *in vitro* analyses or for 24 hrs before implantation into NSG mice. (**B**) Flow cytometry analyses of total cells generated from aggregates in vitro after 2 and 4 weeks. (**C**) Photo of a human thymic aggregate in the inguinal region of an NSG mouse at week 5 post-implantation (blue arrow), and flow cytometry analysis of total cells generated from the implanted thymic aggregate in vivo.

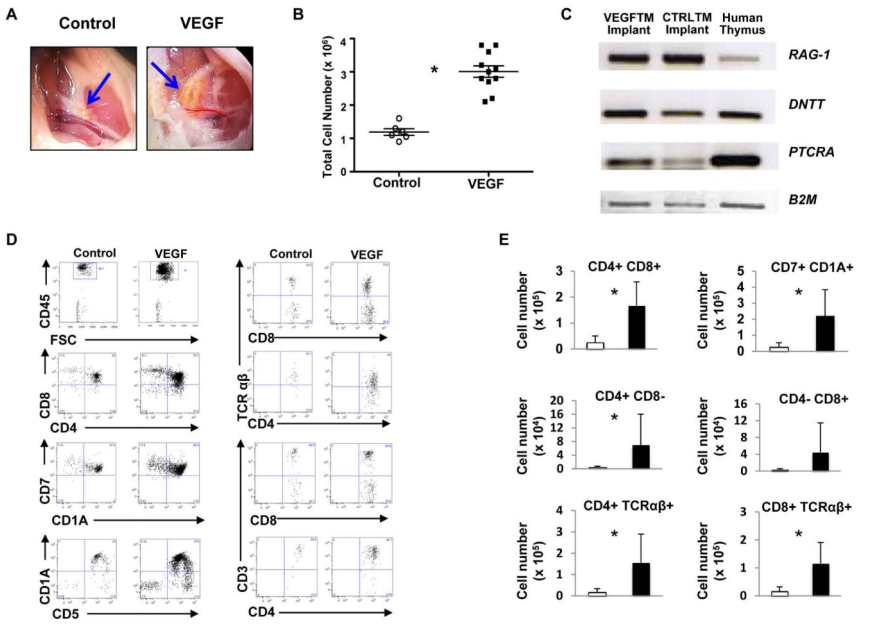

Figure 3. VEGF expression enhances production of human T cells in implanted thymic aggregates

Analyses of human thymic aggregates at day 35 post-implantation are shown. (**A**) Photo of implanted thymic aggregates (blue arrows) immediately prior to harvest from the inguinal region. The VEGF-expressing thymic aggregates were larger and displayed more vigorous vascular growth than that of the control aggregate. (**B**) Total cell number in aggregates with detectable hCD45+ cells. (*$P< 0.002$, two- tailed t test with unequal distributions; Control N=6/11, VEGF N=11/17 mice with implants recovered). (**C**) Implanted thymic aggregates expressed genes critical for early stages of thymopoiesis. Equal amounts of mRNA derived from each aggregate and fresh postnatal human thymocytes were analyzed by semi-quantitative RT-PCR. Human beta 2 microglobulin (HB2-M) was used as loading control. (**D**) Human CD45+ cells (gated as shown top left) were further analyzed by FACS for the expression of T cell markers shown (**E**) The number of human CD4+CD8+ ($P< 0.0004$), CD7+CD1A+ ($P< 0.003$), SP CD4+CD8−($P< 0.04$), SP CD4-CD8+, CD4+TCRαβ ($P< 0.0006$), and CD8+TCRαβ ($P< 0.002$) cells was significantly higher in VEGF implants than control (two- tailed t test with unequal distributions).

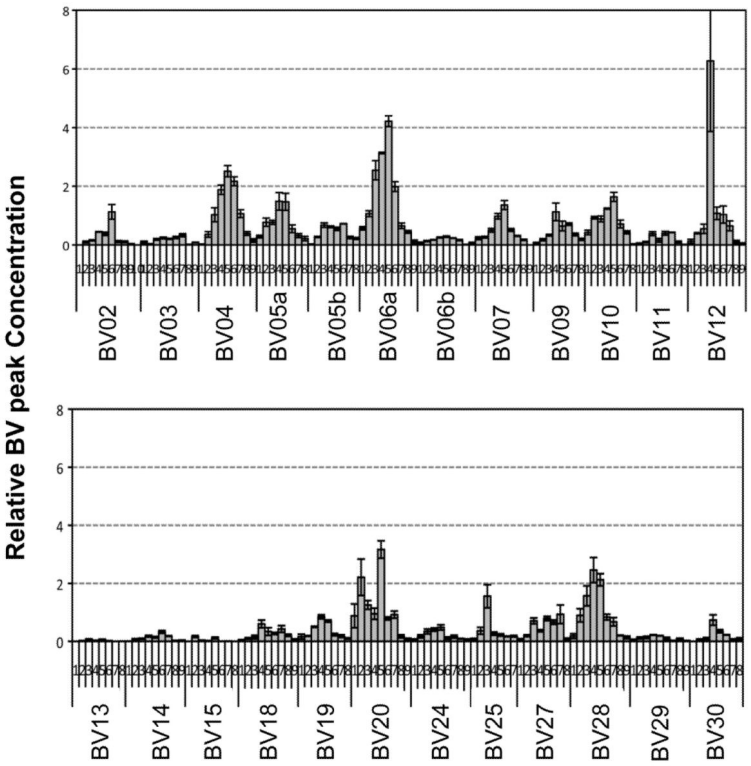

Figure 4. T cell receptor repertoire of thymocytes harvested from thymic implants

Human T cells derived from CB CD34+ cells 5 week after implantation of VEGF expressing thymic implants undergo normal V(D)J TCR chain recombination. Based on quantitative PCR-based TCR spectratyping analyses of human specific CDR3 length distribution of V_β chain families, T cells generated from the implanted thymic aggregate displayed broad distributions of V_β chain fragments (data is displayed across two panels of different V_β chains).

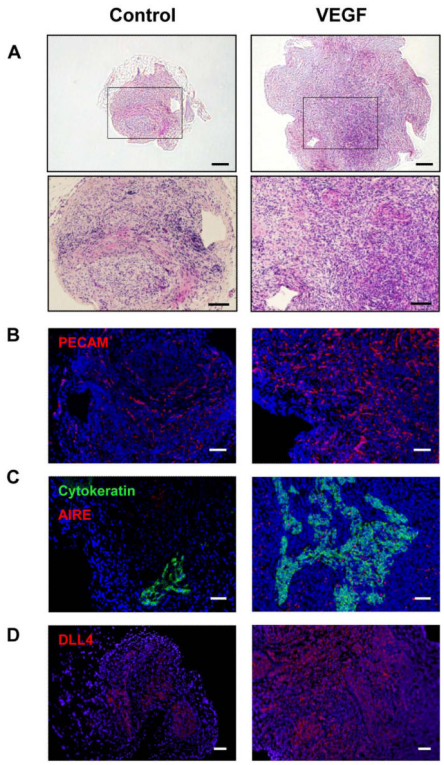

Figure 5. Histological analysis of implanted thymic aggregates

Shown are representative tissue sections from implanted control and VEGF thymic aggregates. (**A**) H&E staining of representative human thymic implant tissue samples. Scale bars = 200μm (100μm in insert). Tissue sections from each group were analyzed for expression of **(B)** PECAM (red), Scale bars = 200 μm, (**C**) pan-cytokeratin (green) and AIRE (red), Scale bars = 100 μm, and **(D)** DLL4 (red), Scale bars = 200 μm. b-d, DAPI (blue) staining of nuclei. See “Materials and methods, Histologic analyses” for image acquisition information.

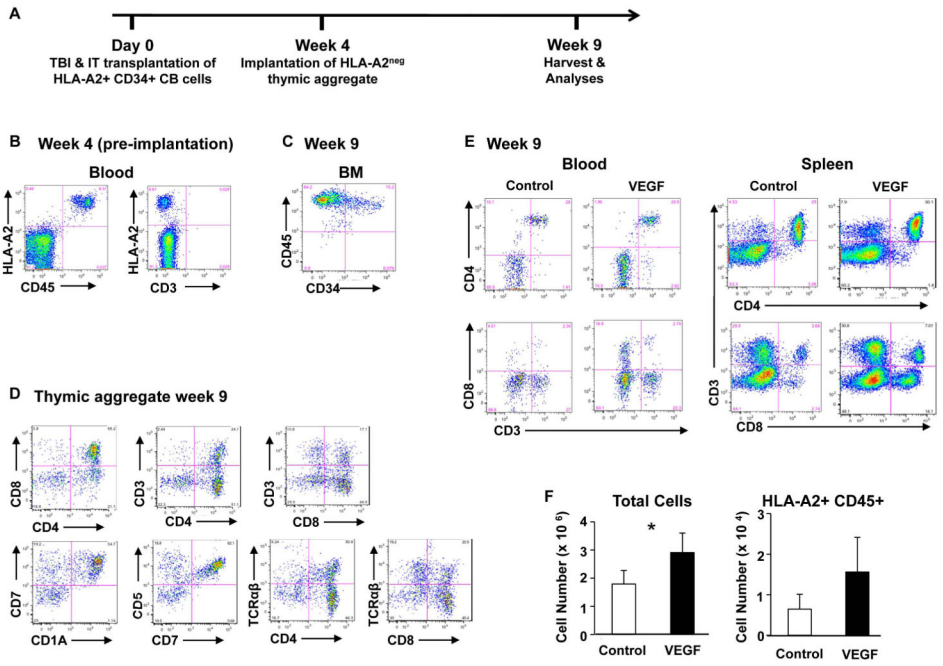

Figure 6. HSPC are recruited from the bone marrow to implanted thymic aggregates and develop into T cells

(**A**) Schematic diagram of the experimental design. Following 250 cGy total body sublethal irradiation (TBI), 8-10 week old NSG mice received transplants of 3×10^5 HLAA2+ CB CD34+ HSPC intra-tibially. Four weeks after HSPC transplantation (HSPCT), peripheral blood (PB) was analyzed by FACS, and then control and VEGF thymic aggregates mixed with HLA-A2 negative CB CD34+ cells were implanted under the quadriceps muscle sheath of recipient animals. 5 weeks after implantation (9 weeks after HSPC transplantation), tissues were harvested for analysis. (**B**) Representative FACS analyses four weeks after HSPC transplantation showing $CD3^{neg}$HLA-A2+ cells in peripheral circulation. (**C-E**) FACS analysis 5 weeks after implantation (9 weeks after HSPC transplantation) of (**C**) BM from implanted mouse, on cells initially gated as HLAA2+; (**D**) VEGF expressing thymic aggregate, gated on HLA-A2+ CD45+ cells; (**E**) blood and spleen from control and VEGF-implanted animal showing phenotype of peripheral human T cells. Phenotypic markers on cells were initially gated as HLA-A2+ CD45+. (**F**) The total and HLA-A2+ CD45+ human mean cell numbers in aggregates are shown 5 weeks after implantation (9 weeks post HSPCT).* significant differences between control and VEGF ($P< 0.05$) (two- tailed t test with unequal distributions, Control N=3, VEGF N=4).